ELSEVIER

Journal of Chromatography A, 855 (1999) 273–290

JOURNAL OF CHROMATOGRAPHY A

www.elsevier.com/locate/chroma

Capillary columns with in situ formed porous monolithic packing for micro high-performance liquid chromatography and capillary electrochromatography

Isabelle Gusev, Xian Huang, Csaba Horváth*

Department of Chemical Engineering, Yale University, P.O. Box 208286, New Haven, CT 06520-8286, USA

Received 13 April 1999; received in revised form 17 May 1999; accepted 1 June 1999

Abstract

Capillary columns with monolithic stationary phase were prepared from silanized fused-silica capillaries of 75 μm I.D. by in situ copolymerization of divinylbenzene either with styrene or vinylbenzyl chloride in the presence of a suitable porogen. The porous monolithic support in this study was used either directly or upon functionalization of the surface to obtain a stationary phase that was appropriate for the separation of peptides by capillary electrochromatography (CEC). The main advantages of monolithic columns are as follows. They do not need retaining frits, they do not have charged particles that can get dislodged in high electric field, and they have relatively high permeability and stability. Whereas such columns are designed especially for CEC, they find application in micro high-performance liquid chromatography (μ-HPLC) as well. Five different porogens were employed to prepare the monolithic columns that were examined for permeability and porosity. The flexibility of fused-silica capillaries was not adversely affected by the monolithic packing and the longevity of the columns was satisfactory. This may also be due to the polymerization technique, which resulted in a fluid-impervious outer layer of the monolith that precluded contact between the fused-silica surface and the liquid mobile phase. For the most promising columns, the conductivity ratios and the parameters of the simplified van Deemter equation, both in μ-HPLC and CEC, were evaluated. It was found that the efficiency of the monolithic columns in CEC was significantly higher than in μ-HPLC in the same way as observed with capillary columns having conventional particulate packing. This is attributed to the relaxation of band-broadening with electroosmotic flow (EOF) with respect to that with viscous flow. It follows then that the requirement of high packing uniformity to obtain high efficiency may also be relaxed in CEC. Angiotensin-type peptides were separated by CEC with columns packed with a monolithic stationary phase having fixed *n*-octyl chains and quaternary ammonium groups at the surface. Plate heights of about 8 μm were routinely obtained. The mechanism of the separation is based on the interplay between EOF, chromatographic retention and electrophoretic migration of the positively charged peptides. The results of the complex migration process, with highly nonlinear dependence of the migration times on the organic modifier and the salt concentration, cannot be interpreted within the framework of classical chromatography or electrophoresis.

Keywords: Electrochromatograph; Monolithic capillary column; Electroosmotic flow; Proteins; Peptides; Poly(styrene–divinylbenzene)

1. Introduction

Capillary electrochromatography (CEC) with

*Corresponding author. Tel.: +1-203-432-4357; fax.: +1-203-432-4360.

E-mail address: csaba.horvath@yale.edu (Cs. Horváth)

0021-9673/99/$ – see front matter
PII: S0021-9673(99)00697-4

fused-silica capillary columns and electroosmotic flow (EOF) of the mobile phase has attracted interest recently as a new liquid phase analytical separation technique [1–3]. Most separations have been carried out so far using capillary columns packed with alkyl-silica particles [1–14] that have been developed for and used in high-performance liquid chromatography (HPLC), although the need of novel columns especially designed for CEC was recognized some time ago [15]. This kind of column must not only have appropriate chromatographic retention properties but also fixed charges at the surface in order to generate EOF and be stable under the conditions employed in CEC, e.g., in a high electric field. The Achilles heel of present CEC columns is the frit used to retain the particulate packing in the capillary [4,5]. Therefore, a column design that casts off retaining frits would be highly desirable [15]. Furthermore, particles of the charged stationary phase may be dislodged in packed columns under the influence of the high electric field, with concomitant changes in column properties [16,17]. The use of open tubular columns [18–21] or columns packed with a stationary phase that can be considered as a single piece, i.e., having a monolithic porous structure, have been suggested to overcome these problems. Such monolithic porous structures are formed in situ by polymerization or consolidation of particulate packings [22–24].

Employment of 'consolidated' packing and a process for the consolidation of the particles of column packing was suggested for gas chromatography in 1966 [25]. A few years later, monolithic column packings were prepared for gas and liquid chromatography by in situ formation and agglomeration of polyurethane particles in a steel tubing [26–28]. In the late 1980s, compressed continuous polymer gel beds prepared by in situ polymerization of an aqueous solution of acrylamide derivatives were introduced [29]. 'Molded' continuous rods, prepared by in situ polymerization of styrene–divinylbenzene, were introduced for reversed-phase HPLC [30]. Continuous rods of molecularly imprinted polymers, prepared in situ, were used for chiral separations [31]. Recently, siliceous 'continuos supports' were prepared by the sol-gel process [32].

In situ polymerization yields columns that have higher porosities and permeabilities than obtained using conventional packing with particulate stationary phases, without altering column stability. Nonetheless, their use in liquid chromatography columns of traditional dimensions have not found significant practical applications. Most problems with traditional monolithic columns arise from radial non-uniformity associated with the fabrication and from axial non-uniformity, e.g., gaps, due to instability of the packing. The wider the column is, the greater is such non-uniformity and its untoward effect on the column's efficiency.

Thus, the advent of fused-silica capillary columns (20–100 μm I.D.), first in gas chromatography and then in CEC, has offered an opportunity to reexamine the validity of monolithic packings in columns of such small inner diameter. Therefore, in situ preparation of monolithic packings in fused-silica capillaries led to packed capillaries without the shortcomings of traditional columns [15]. In CEC, fused-silica capillaries with a cross-linked thick gel prepared by in situ polymerization of acrylamide derivatives were introduced as a 'fritless' continuous bed [33–35]. In these columns, air bubbles seldom formed, due to the absence of retaining frits. Recently, capillary columns with a rigid porous 'continuous rod' for reversed-phase CEC were prepared by copolymerization of acrylic monomer and crosslinking agent in the presence of a porogen inside raw fused-silica capillaries [36]. Using sol-gel technology, a porous glass matrix (xerogel) was prepared in capillary columns for reversed-phase CEC of uncharged organic compounds [37,38].

From the above discussion, it is evident that many avenues have already been explored regarding the preparation and use of a variety of monolithic, i.e. consolidated column packings in chromatography. In view of the most likely prospect that capillary columns with monolithic packing will be widely employed in CEC and μ-HPLC, we offer the following definition for a monolithic stationary phase. A monolithic stationary phase is a continuous unitary porous structure prepared by in situ polymerization or consolidation inside the column tubing and, if necessary, the surface is functionalized to convert it into a sorbent with the desired chromatographic binding properties. A schematic illustration of monolithic column packing in capillaries is presented in Fig. 1.

Previously, we prepared in situ a porous styrenic

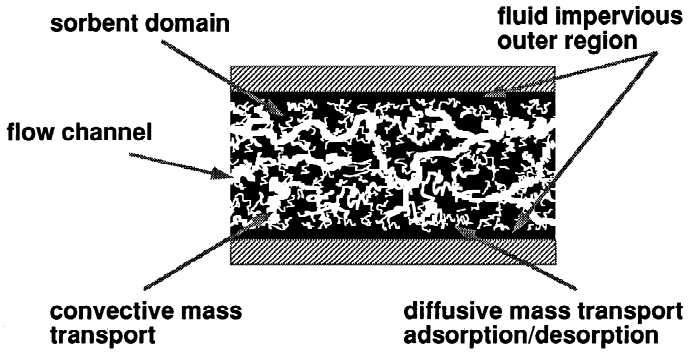

Fig. 1. Schematic illustration of a monolithic packing prepared by in situ copolymerization of styrene and divinylbenzene in a fused-silica capillary with a silanized inner wall.

monolithic packing inside a 530 μm I.D. capillary to separate standard proteins by reversed-phase μ-HPLC with gradient elution at elevated temperature [15]. In this study, our goal was to investigate the conditions of in situ formation of an appropriate bimodal porous support that has relatively high Darcy's law permeability. The porous monolithic supports were characterized and, in order to obtain a stationary phase that was suitable for the separation of peptides by CEC, the surface was functionalized.

2. Experimental

2.1. Materials

Tri-peptides, Gly–Gly–Phe and Phe–Gly–Gly, standard proteins and synthetic angiotensins were obtained from Sigma (St. Louis, MO, USA). Fisher (Fair Lawn, NJ, USA) supplied thiourea and HPLC-grade acetonitrile, methanol and acetone, analytical-grade phosphoric acid and sodium hydroxide, whereas monobasic, dibasic and tribasic sodium phosphate and dimethylformamide (DMF) (99.9%) were from J.T. Baker (Phillipsburg, NJ, USA). Dimethyl sulfoxide (DMSO) was purchased from Burdick and Jackson (Muskegon, MI, USA), γ-(trimethoxysilyl)propyl methacrylate was from Polysciences (Warrington, PA, USA), 2,2-diphenyl-1-picrylhydrazyl hydrate (DPPH) was from Aldrich (Milwaukee, WI, USA), styrene was from Fluka (Ronkonkoma, NY, USA), divinylbenzene (DVB) (85%) and vinylbenzyl chloride (VBC) were from Dow (Midland, MI, USA), and azobisisobutyronitrile (AIBN) (98%) was from Pfaltz and Bauer (Waterbury, CT, USA). Hydrofluoric acid (48%) was of analytical reagent grade from Mallincrodt (Paris, KY, USA). Fused-silica capillaries (75 μm I.D. and 375 μm O.D.) with polyimide cladding were purchased from Quadrex (Woodbridge, CT, USA). Styrene and DVB were washed with 10% (w/v) aqueous sodium hydroxide to remove the inhibitors before use. The toluene and acetone were anhydrous and were stored in the presence of dehydrated activated molecular sieves (Fisher). The sodium phosphate buffers were prepared by diluting a 20-m*M* stock solution to the desired concentrations with appropriate volumes of water and acetonitrile. The mobile phases were degassed by ultrasonication and were filtered through an organic filter (pore size=0.2 μm). Deionized water, which was used throughout, was prepared using a NANOpure purification system (Barnstead, Boston, MA, USA).

2.2. Instrumentation

2.2.1. μ-HPLC unit

μ-HPLC experiments were performed using a modified Hewlett-Packard (Wilmington, DE, USA) HP 1090 Series liquid chromatograph, equipped with an autosampler, a Model DR5 solvent delivery system, a Model 2000 UV detector with a Model 9550-0155 on-column capillary cell (Thermo Separation Products, Fremont, CA, USA). Control of the chromatographic system and data acquisition were performed by a HP ChemStation System (Hewlett-

Packard), product number G2170AA. The flow from the HPLC instrument was split after the injection valve using a stainless steel TEE-piece (Valco, Houston, TX, USA) connected to a restriction capillary. The split ratio was typically about 10 000:1 and could be adjusted by the length and diameter of the capillary restrictor.

2.2.2. Laboratory-made CEC unit

The CEC experiments were carried out in a laboratory-made apparatus, equipped with a Model SpectraFOCUS detector and a Model 9550-0155 on-column capillary cell (Thermo Separation Products) [10]. The unit was modified by grounding the outlet electrode to keep the zero voltage at the column's detection side. The 30 kV bipolar power supply (Spellman, Plainview, NY, USA), which was connected to the inlet electrode, allowed for a reversible polarity. A freshly made column was always equilibrated with the mobile phase overnight. Later, when a different mobile phase was introduced, the column was rinsed for ca. 1 h by applying a nitrogen gas pressure of 120 p.s.i. (1 p.s.i.=6894.76 Pa) at the inlet vial, followed by electrokinetic equilibration at 5 kV for 30 min, or until a stable base line was attained.

The samples were injected electrokinetically for 2 s at a voltage of 2 kV. If not otherwise stated, separation was performed at an applied voltage of 15 kV with cathodic EOF for unfunctionalized monolithic columns and anodic EOF for columns with quaternary ammonium groups at the chromatographic surface. Between runs, the column was rinsed with the mobile phase for 10 min at an inlet pressure of 120 p.s.i. All experiments were carried out at room temperature, and both the inlet and the outlet of the column were kept at atmospheric pressure.

2.2.3. Microscopy

Visual examination of the fused-silica capillaries was performed using an optical Olympus BH-2 (Olympus Corporation, Woodbury, NY, USA) microscope, by the transmitted light illumination method with typically 100-fold magnification. The Model ISI SS-40 scanning electron micrograph (International Scientific Instruments, Santa Clara, CA, USA) was operated at 10 kV and at a filament current of 40 mA. The specimens were fractured and cut into ca. 2-mm-long pieces. Some of the fragments were immersed in aqueous hydrofluoric acid (48% HF) for 10 min, in order to dissolve the fused-silica tubing and, thus, to unsheathe the monolith. After rinsing with water, the specimens were dried and mounted, by placing them first on an aluminum stub via a double-sided carbon tape (Electron Microscopy Sciences, Ft. Washington, PA, USA). Then, they were sputter-coated with a gold/palladium alloy using an SPI Sputter (SPI Supplies Division of Structure probe, West Chester, PA, USA) for 25 s at 30 mA, to prevent charging.

2.2.4. Liquid porosimetry

The pore volume distributions of the samples were determined in the pore size range 1–1000 μm by the diaphragm method [39] using a TRI Autoporosimeter (TRI, Princeton, NJ, USA) [40]. For measurements with this instrument, the specimen was first immersed in hexadecane and then placed on a membrane in a chamber that was pressurized by nitrogen. Upon increasing the gas pressure within the chamber in a stepwise manner, the liquid was displaced by the gas from the pores, beginning with the largest pores. A top-loading recording balance measured the amount of liquid removed from the sample as a function of the applied pressure.

3. Column preparation

3.1. Silanization of the capillary's inner wall

Siloxane groups at the inner surface of raw fused-silica capillaries were hydrolyzed first in order to increase the density of silanol groups serving as anchors for the subsequent silanization. A 75-μm I.D. capillary was washed and filled with 1 *M* NaOH solution, sealed at both ends using a butane flame burner (Veriflo Air-Gas Torch, Macalaster Bicknell, New Haven, CT, USA) and heat-treated in an oven at 120°C for 2 h. Thereafter, the capillary was washed with ca. 50 column-volumes of deionized water and then with the same volume of acetone. Subsequently, the capillary tube was purged at 120°C with nitrogen for 1 h, to dry it.

The inner wall of the fused-silica capillary was treated with the heterobifunctional coupling agent

γ-(trimethoxysilyl)propyl methacrylate in order to provide anchoring sites for the grafting of the polymer to the silica surface and enhance wetting of the surface by the styrenic monomer mixture. The reaction of the trimethoxysilyl moiety of the heterobifunctional silanizing agent, γ-(trimethoxysilyl)propyl methacrylate, with the silanols at the fused-silica surface is preferentially carried out at elevated temperatures [41]. However, at high temperatures, polymerization of the reagent via the vinyl groups occurs. In order to slow down the polymerization, the inhibitor DPPH was added to the reaction mixture [42]. The effect of using the inhibitor is evident from the comparison of the attachment of the monolith to the fused-silica capillary wall, which is shown in Figs. 2A and 3A. It is seen that, in the reaction without the inhibitor (Fig. 2A), there is a cleft between the monolith and the inner wall of the capillary, whereas in the presence of the inhibitor, the monolith is attached to the capillary's inner wall. After testing a large set of conditions, treatment at 120°C and the use of the inhibitor DPPH were found to give the most stable packing.

A solution of 50% (v/v) of the silanizing agent in DMF containing 0.01% (w/v) of the inhibitor DPPH was prepared and purged with helium for 10 min. The capillary was rinsed with ten column-volumes of the solution and both ends of the capillary were sealed. Subsequently, the sealed tube was heated in an oven at 120°C for 6 h, and then was cooled to room temperature and washed with ca. 50 column-volumes of acetone and dried with a nitrogen stream. In most cases, 3–5 m lengths of the fused-silica capillary were treated in these procedures. The quality of surface treatment was judged by the value of the contact angle of water, determined by the capillary rise method, as discussed elsewhere [42]. Only silanized capillaries with contact angles of 70° and greater were used for preparing monolithic packings.

The scanning electron micrographs presented in Fig. 3 illustrate that silanization facilitates a strong attachment between the silica surface and the styrenic monolith. We believe that this is due to the formation of a fluid-impervious annular outer layer of the polymeric monolith at the silanized fused-silica surface. This layer precludes contact between the mobile phase and the inner wall of the fused-silica capillary, as already discussed in the literature [42] and, thus, imparts stability to the columns. As a control, the monolith was polymerized also in un-silanized fused-silica capillaries. As expected, in this case, the monolith did not adhere to the capillary wall, as shown in Fig. 2B, and was easily removed by rinsing the column with a 0.1-*M* solution of sodium hydroxide at a pressure drop of 30 p.s.i.

3.2. Preparation of a porous monolithic support

The PS–DVB monolith is formed inside the capillary by in situ polymerization of a styrene–divinylbenzene mixture in the presence of a suitable porogen [43]. Ideally, the porous monolith is bimodal, as illustrated schematically in Fig. 1. It consists of channels for mobile-phase flow as well as of domains with relatively small pores, which provide most of the adsorption capacity of the column and can be reached only by molecular diffusion. The formation of a bimodal pore structure requires the use of more than one porogen and the composition of the porogen mixture is critical for the preparation of optimal column packing. In contrast to classical suspension polymerization in aqueous medium, where only water-immiscible porogens can be used, our polymerization method inside the capillary also allows the employment of water-miscible porogens. Consequently, it offers a greater degree of freedom in choosing the porogen and, for that matter, in designing the polymerization procedure.

To prepare monolithic columns with different porous structures, the polymerization was carried out under the conditions listed in Table 1. The styrene to divinylbenzene ratio was kept in the vicinity of 2:1. Typically, four parts of the monomer mixture were mixed with six parts of an alcohol or an alcohol mixture, which was used as a porogen. The mixture contained 0.1% (w/v) of the initiator AIBN. The solution then was purged for 10 min by flowing helium through a silanized capillary, which was used thereafter for the preparation of the monolithic column. The capillary was disconnected from the gas supply and was filled up with the monomer mixture. The capillary was either filled up completely or only up to a certain distance from one end. Thus, monolithic columns could be prepared with or without an open segment. After sealing both ends of the capil-

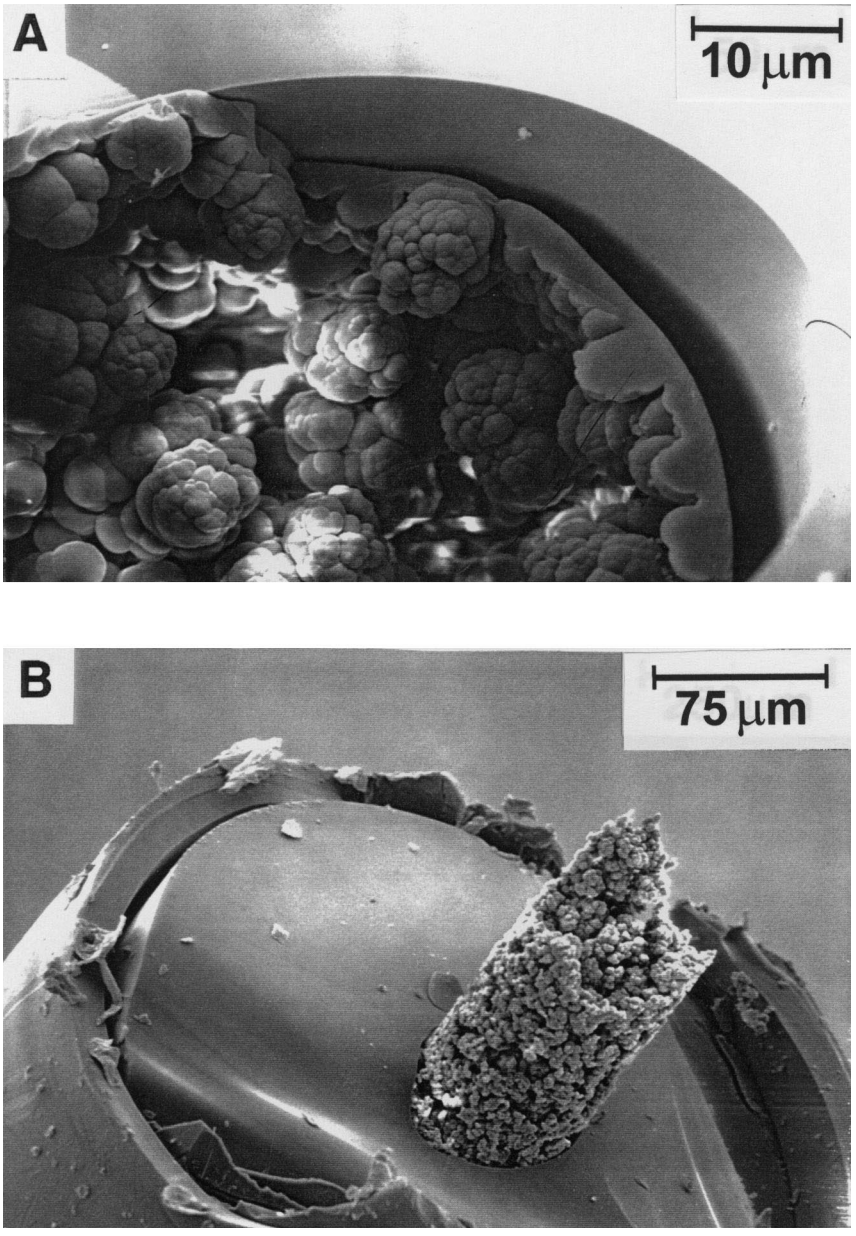

Fig. 2. Effect of improper pretreatment or no pretreatment of the fused-silica capillary on the attachment of the monolith to the capillary's inner wall. (A) The inner wall was silanized without an inhibitor and (B) the inner wall was not silanized.

lary, the polymerization was allowed to proceed for 24 h in a water bath thermostated at 70°C.

In the process, a highly crosslinked porous monolith, which is bonded to the silanized wall of the capillary, is formed. As shown by the scanning electron micrograph in Fig. 3A, the polymeric

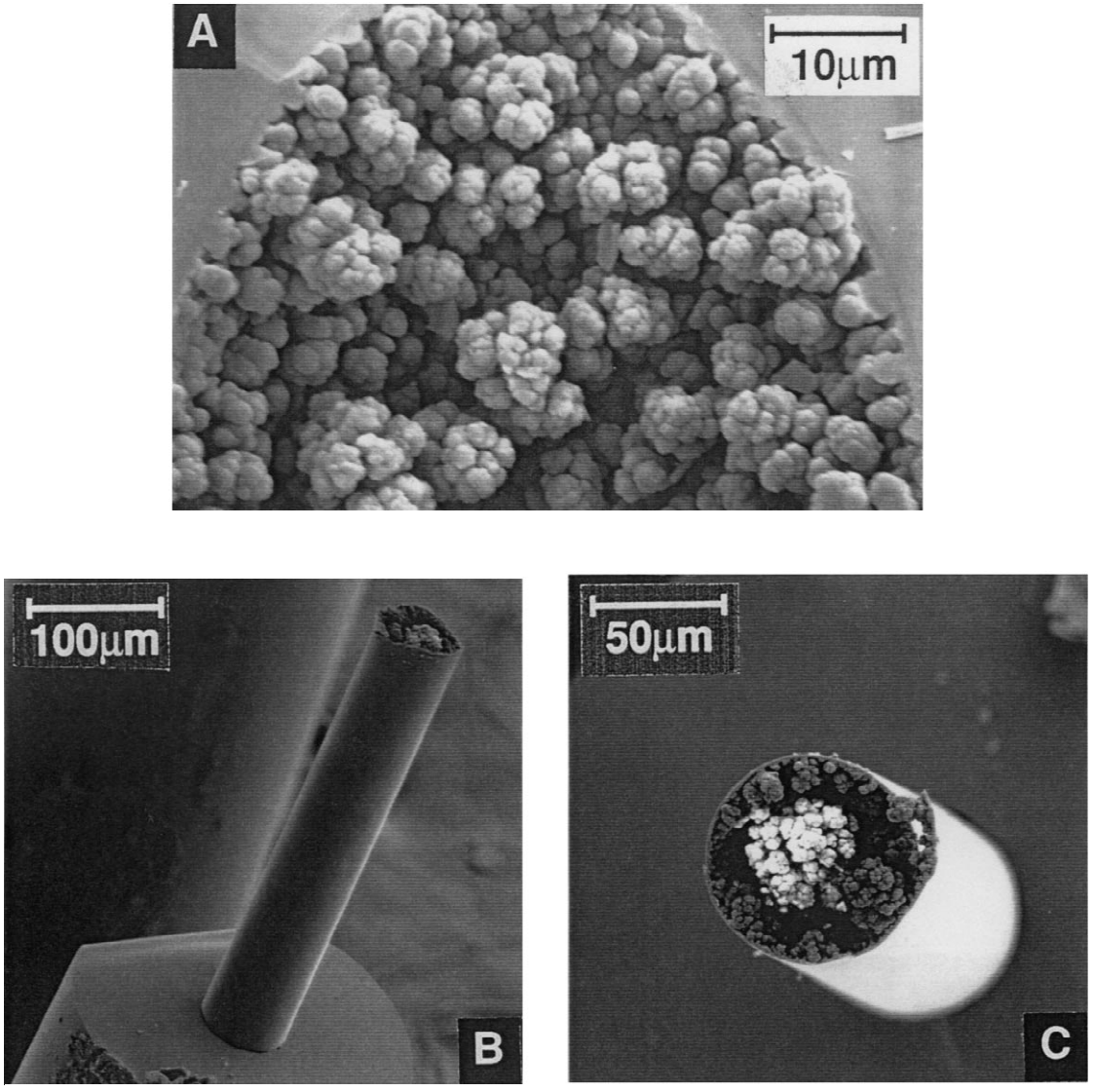

Fig. 3. Scanning electron micrographs of monolithic packing in a fused-silica capillary of 75 μm I.D. with the inner wall pretreated with γ-(trimethoxysilyl)propyl methacrylate containing the inhibitor DPPH. The specimens were first fractured and then (A) the fractured ends were cut into ca. 2 mm-long pieces or (B) and (C) they were partially immersed in aqueous hydrofluoric acid (48% HF) for 10 min, to remove the fused-silica, and then washed with water and cut to a length of ca. 2 mm.

stationary phase consists of small globuli that are slightly fused together into a single piece to form a rigid yet highly permeable monolithic support.

Once the polymerization was completed, column ends were opened and the column was purged with nitrogen at 200 p.s.i. for 1 h in order to remove volatiles. The column then was washed with acetonitrile, using a pressure of 60 p.s.i. from a nitrogen cylinder, dried and stored in a glass tube of 5 mm I.D. The in situ polymerization of each monomer

Table 1
Effect of polymerization conditions on the total porosity, ε_T, permeability, B°, and the impedance of the columns, ψ, with styrenic monolith, using AIBN as an initiator

Column number	Ratio of styrene–divinylbenzene in the monomer mixture	Porogen 60% (v/v)	Temperature °C	ε_T	B° [Darcy]	ψ
I[a]	STY/DVB 2:1	Ethanol Water Methanol	4 h @ 75°C, followed by 20 h @ 80°C	0.41	0.57	380
II[a]	STY/DVB 1:1	Ethanol Water Toluene	24 h @ 70°C	0.65	0.91	4700
III[a]	STY/DVB 2:1	Ethanol	24 h @ 70°C	0.62	0.858	
IV[a]	STY/DVB 2:1	*n*-Propanol	24 h @ 70°C	0.65	1.28	1200
V[a]	VBC/DVB 1:1	*n*-Propanol Formamide	3 h @ 65°C, followed by 37 h @ 75°C	0.45	0.184	
VI[b]	VBC/DVB 1:1	*n*-Propanol Formamide	3 h @ 65°C, followed by 37 h @ 75°C	0.45	0.184	

[a] Porous monoliths without functionalization.
[b] The porous monolith was functionalized with octyl- and trimethylammonium groups.

mixture listed in Table 1 was carried out in duplicate.

About 2 ml quantities of the monomer mixture for Column III and Column IV were polymerized in glass vials into a porous monolith. The polymeric samples so prepared were washed with acetone to remove any soluble compounds, vacuum dried at 60°C for 4 h, examined visually under the microscope and subjected to porosimetry.

3.3. Functionalization of the monolithic support

The stationary phase in CEC should meet several, often contradictory, requirements. The surface of the solid support has to have fixed charges to generate EOF in a high electric field. The magnitude of the EOF velocity depends, according to von Smoluchowski [44], on the zeta potential of the packing surface and the electric field strength.

In order to have reactive groups on the surface of the porous polymeric stationary phase, the monolithic support was prepared by in situ copolymerization of vinylbenzyl chloride (VBC) and DVB in the presence of a *n*-propanol–formamide mixture that served as the porogen. Subsequently, it was in situ functionalized by reacting the chloromethyl groups at the surface with *N*,*N*-dimethyloctylamine. Thereafter, columns were washed with methanol and equilibrated with the mobile phase.

3.4. Making the detection window

A 2–3-mm segment of the column, at a distance of 10 cm from the outlet end, was heated with an Archer Torch Model B, which is a microtorch that is fueled with butane (Radio Shack, New Haven, CT, USA), while the column was purged with oxygen at an inlet pressure of 120 p.s.i. By this treatment, the polyimide outer coating was burned off and the monolithic packing was pyrolized. The volatile products of the pyrolisis cum oxidation reaction were removed from the column by the stream of oxygen. Subsequently, the column was washed with about 100 column-volumes of acetonitrile. In most cases, the preparation of the detection window was the last step in the preparation of the column.

4. Column characterization

4.1. Porosity of the monolith

The porous structure of the monolithic packings in capillary columns is characterized by methods developed by geologists and reservoir engineers for rock samples, although the very small dimensions of the monolithic capillary packing are the source of experimental difficulties. Three methods are used: the flow method, employing a μ-HPLC system, the conductivity method under CEC operation conditions and the gravimetric method.

The flow method employs an inert tracer, which explores both the interstitial and intraparticulate spaces of the stationary phase. The velocity of the inert tracer is the chromatographic velocity, which is distinctly different from the interstitial and superficial flow velocities that are used in the study on the flow through porous media [10,45]. It must be noted here that the unique architecture of monolithic columns does not allow for distinguishing between intra- and interparticular spaces of the packing so that the original concept of interstitial flow velocity does not apply to this type of column without modification.

In the flow method, the mobile-phase velocity was measured with the μ-HPLC unit by an inert tracer and the volumetric flow-rate was also measured. Then, with the known empty tube volume, the total porosity, ε_T, of the monolith was calculated following the literature method [45]. The measurements at different flow-rates yielded average values of the total porosity, as shown in Table 1. The porosities of columns II, III and IV are nearly the same and equal the volume fraction of the porogen in the monomer mixture.

The electrical conductivity method developed in reservoir engineering [46] for estimation of the total porosity of monolithic samples is applicable when the porous stationary phase is nonconducting. Then, the conductivity method can be employed to our monoliths as well. In this approach, a dimensionless parameter, the so called 'formation resistivity factor', is used. In CEC, the term conductivity ratio, the reciprocal of formation factor, is used mainly to estimate the porosity of the packing. In order to evaluate the conductivity ratio, the monolithic column and an open tube of exactly the same dimensions are filled with a suitable electrolyte solution. Then, the conductivity of both tubes is measured and the conductivity ratio, which is, by definition, smaller than unity, is calculated.

Table 2 lists the most common equations derived for the dependence of the conductivity ratio, ϕ, on the total column porosity. The equations are illustrated by double logarithmic plots in Fig. 4, together with three data points obtained with three monolithic columns using the flow method. As seen in Fig. 4, Archie's simple power law offers the closest fit of the experimental data. It is believed that the exponent, 1.3, called the cementation factor, gives information on the tortuosity and interconnectivity of the pore network. Further support for the applicability of the conductivity method has been gained from subjecting Column III to porosimetry by using the gravimetric method. In this method, the porosity was determined from the density of acetone and the weight difference between the dry and acetone-filled monolithic column, as measured with a differential Cahn balance (Cahn Instruments, Madison, WI, USA). The values of the total porosity for Column III obtained by the three methods matched very well within the experimental error. The results presented in Table 3 and Fig. 4 suggest that the conductivity ratio, which is rather easy to determine experimentally, offers a suitable method for the characterization of the monolithic column packings in CEC.

4.2. Mean pore radius of the monolith

The pore-size distribution of two samples obtained by bulk polymerization with different porogens corresponding to those used for Columns III and IV was determined by liquid extrusion porosimetry with

Table 2
Dependence of the conductivity ratio, ϕ, on the total porosity, ε_T

Name	Equation	Reference
Tobias	$\phi = \varepsilon_T^{1.5}$	[47]
Archie	$\phi = \varepsilon_T^{1.3}$	[48]
Wyllie	$\phi = \varepsilon_T / \sqrt{2}$	[49]
Humble	$\phi = 1.613\varepsilon_T^{2.15}$	[50]
Slawinski	$\phi = \varepsilon_T / (11.3219 - 0.3219\varepsilon_T)^2$	[51]

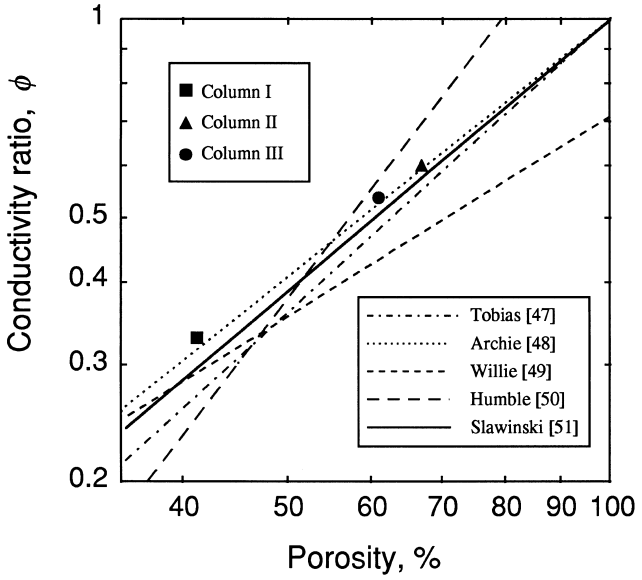

Fig. 4. Plots showing the dependence of the conductivity ratio on the column porosity according to the various relationships found in the literature for the determination of the porosity by the conductivity method. The three data points illustrated were obtained experimentally with three monolithic columns.

hexadecane [40], as described above in the Instrumentation section. The resulting integral pore volume distribution curves are shown in Fig. 5. It is seen that the median pore radius for a monolithic sample prepared with ethanol as the porogen is ca. 5 μm, in agreement with the value estimated from the scanning electron microscope (SEM) micrograph shown in Fig. 3. In contrast, the mean pore radius of the specimen prepared under identical conditions but with *n*-propanol as the porogen was found to be ca. 7 μm.

4.3. Column permeability

The Darcy's law permeability of a porous medium is a measure of its capacity to transmit a fluid driven by an imposed pressure drop. By analogy with electrical conductance, it represents the reciprocal of the resistance to flow by the porous medium [52]. The specific permeability of the column was determined by forcing acetonitrile through the column at different flow-rates in the inlet pressure range from 40 to 400 bar using a Model SFC-500 syringe pump (ISCO, Lincoln, NE, USA). Darcy's law holds with viscous flow and leads to the definition of the specific permeability of the column, B°, as

$$B^\circ = \eta \cdot L \cdot Q/A \cdot \Delta P \quad (1)$$

where η is the viscosity of the mobile phase, L is the column length, Q is the flow-rate and A is the cross sectional area of the conduit normal to the direction

Table 3
Total porosity of Columns I, II and III measured by the various methods described in Section 4.1

Column	Conductivity method					Flow method	Gravimetric method
	Tobias	Archie	Wyllie	Humble	Slawinski		
I	0.487	0.436	0.481	0.485	0.467	0.41	–
II	0.708	0.672	0.843	0.629	0.712	0.65	–
III	0.662	0.622	0.762	0.601	0.663	0.62	0.67

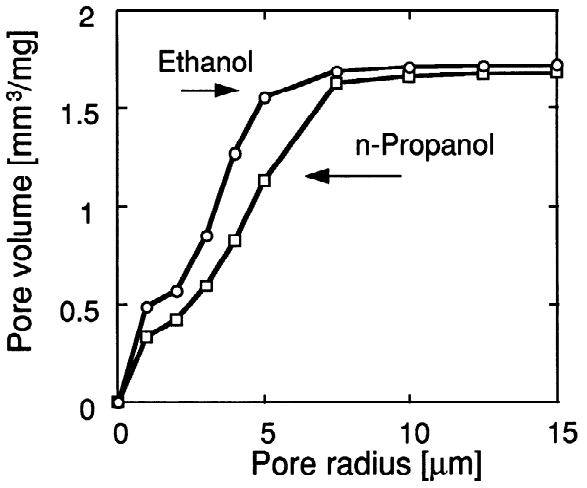

Fig. 5. Integral pore volume distribution of two styrenic monoliths measured by liquid extrusion porosimetry using hexadecane. The polymerization conditions of the monoliths were the same as those used for Columns III and IV with ethanol and *n*-propanol as the porogen, respectively.

of flow [53]. The ratio of Q and ΔP in Eq. 1 was determined from the slopes of the ΔP versus Q plots, as shown in Fig. 6.

The structure and, hence, the permeability of monolithic columns strongly depends on the details of their preparation, as seen in Table 1. Comparison

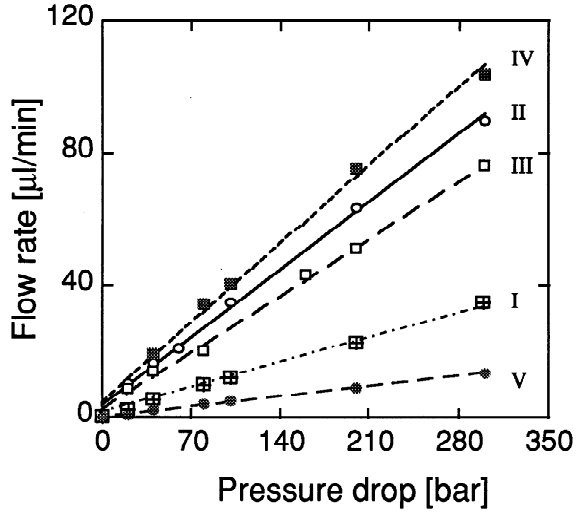

Fig. 6. Plots of the volumetric flow rate of ACN against the applied pressure with monolithic Columns I–V that are described in Table 1.

of the permeabilities of Columns III and IV would suggest that the more hydrophobic the porogen, the more permeable the monolithic structure. Although the porous monolithic packing structure escapes characterization methods used for particulate column packing, the Kozeny–Carman equation [53] is applicable for calculating an effective radius of the equivalent pores from the permeability and porosity. For our purpose, it is written as

$$d_p = 2 \cdot \left(\frac{5 \cdot B^o}{\varepsilon_T} \right)^{1/2} \quad (2)$$

where d_p is mean pore diameter and ε_T is total porosity. The factor, 2, is the shape factor for cylindrical pores and the coefficient, 5, is the empirical Kozeny coefficient for the pore structure. The respective pore radii for Columns III and IV in Table 1 with ethanol and propanol as a porogen were found to be 4.7 and 6.5 μm, which agree well with the data obtained by liquid extrusion porosimetry and with the estimates from the SEM pictures presented in Fig. 3.

4.4. Column efficiency in μ-HPLC and CEC

The peak efficiency of two monolithic columns was examined in both the CEC and μ-HPLC mode by using the same mobile phase and by measuring the band-spreading of thiourea, which was considered to be an unretained tracer under the conditions of the experiment. The plate efficiency was measured using the peak width at half height method and the data were analyzed using the simplified van Deemter equation [54]. van Deemter plots of the data obtained in μ-HPLC and CEC with Columns I and II, vide Table 1, are presented in Fig. 7. As seen, the plate height in CEC plateaus at flow velocities greater than 1 mm/s and this suggests that rapid separations can be obtained with such columns without loss in resolution. The van Deemter parameters A and C are shown in Table 4, together with the attenuation factors, given by the ratio of the A and C terms of the van Deemter equation, measured in HPLC and in CEC, respectively [55]. The attenuation factors all are greater than unity and this is an indication that band-spreading due to the bed nonuniformities and mass transfer resistances is greater with viscous flow

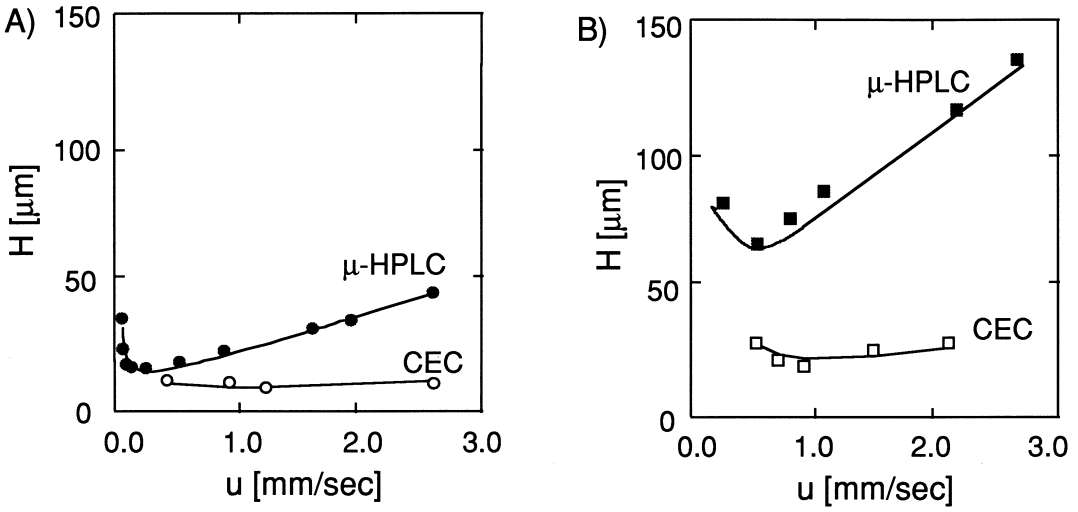

Fig. 7. Van Deemter plots of data obtained with both voltage-driven (CEC) and pressure-driven (μ-HPLC) flow in two monolithic columns prepared with different porogens. (A) Column I (μ-HPLC ●, CEC ○), 75 μm×27/38 cm. (B) Column II (μ-HPLC ■, CEC □), 75 μm×28/38 cm; PS–DVB unfunctionalized monolith. Mobile phase, 10 m*M* sodium phosphate buffer, pH 6.8; detection, 214 nm; sample, thiourea (0.2 mg/ml); electrokinetic injection, 2 s, 2 kV. Columns I and II are described in Table 1.

than with EOF. The poor efficiency of Column II vide Fig. 7B in the HPLC mode is rather surprising and indicates that the packing in this column is highly non-uniform. Comparison of Figs. 7A and 7B reveals the enhancement in column efficiency when viscous flow is replaced by EOF and how the structural properties of monolithic columns can be different depending on the method of preparation. van Deemter plots of angiotensin II and DMSO data obtained with column VI in CEC mode are shown in Fig. 8. The mobile phase contained 50 m*M* NaCl in 10 m*M* sodium phosphate buffer, pH 3.0, and 25% acetonitrile. Plate numbers with the 27/37.5-cm-long column were in the range of 34 000–43 000 with DMSO and 31 000–55 000 with angiotensin. On average, the plate height was approximately 8 μm in the velocity range of the experiment.

Frequently, it is more meaningful to use dimensionless parameters such as the reduced plate height and the reduced velocity, which is also called the Peclet number. In both cases, the particle diameter is used as the characteristic length to obtain the dimensionless quantities. With monolithic column packings, the particle diameter is undefined and the introduction of an 'apparent particle diameter' appears to be of dubious value since it would require unjustifiable assumptions, e.g., a fixed value of porosity. In order to characterize columns in liquid chromatography, the separation impedance, ψ, has been introduced [56]. It is the ratio of the plate

Table 4
van Deemter parameters *A* and *C*, measured with thiourea for Columns I and II in both μ-HPLC and CEC under the same conditions except for the nature of the mobile phase-flow[a]

van Deemter parameters	Column I			Column II		
	μ-HPLC	CEC	Attenuation factor	μ-HPLC	CEC	Attenuation factor
A [μm]	6.391	4.0	1.59	24.0	3.0	8
C [10^{-3} s]	13.843	2.0	6.92	37.95	8.25	4.6

[a] The experimental conditions are described in Fig. 7. The attenuation factor is obtained by dividing *A* in HPLC by *A* in CEC or *C* in HPLC by *C* in CEC.

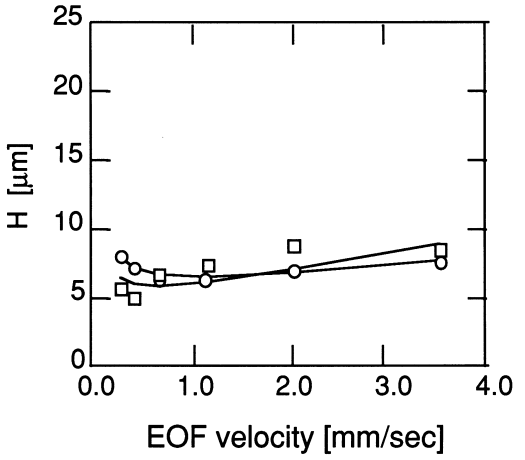

Fig. 8. Plots of plate height of DMSO (○) and angiotensin II (□) against the EOF velocity. Column VI, 75 μm×21/31 cm, porous styrenic monolith with quaternary ammonium and octyl functions; mobile phase, 50 m*M* NaCl in 5 m*M* phosphate buffer with 25% acetonitrile, pH 3.0; reversed polarity; electrokinetic injection, 2 s, 5 kV.

height, squared, and the specific permeability of the column. Both the plate height and the permeability are measurable quantities with columns having monolithic packings. In HPLC, the value of ψ for a good packed column is 2000 with neat aqueous eluents when the column-to-particle diameter ratio is greater than ten and the pressure drop is about 200 bar [57]. In general, monolithic columns are expected to have low ψ values due to their relatively high plate efficiency and permeability. For our monolithic Columns I, II and IV, the separation impedances were approximately 380, 4700 and 1200, as seen in Table 1.

4.6. Column stability

Monolithic column packing should be incompressible under the conditions employed in CEC. Five of our columns were tested for stability by pumping acetonitrile at inlet pressures up to 300 bar in the HPLC unit. The flow-rate as a function of the pressure drop was measured and plotted in Fig. 6. It is seen that the plots are linear, suggesting that the packing was not compressed, even at highest inlet pressure. This test was repeated weekly over a period of two months and the slopes of the plots were reproducible with a relative standard deviation of 3%. In another series of stability testing, the EOF velocity was measured with an inert tracer and 10 m*M* phosphate buffer, pH 7, with similar results. As a third stability test, the conductivity of the column was monitored during each run and was found to be constant over three months of operation. Occasional visual examination by the optical microscope did not show any gaps or other irregularities in the packing after three months of operation with an average current of 40 μA.

5. Chromatographic applications

5.1. Protein separation by μ-HPLC

Column I, which was packed with unfunctionalized porous styrenic monolith, was used to separate four standard proteins by reversed-phase HPLC with gradient elution. The chromatograms shown in Fig. 9 were obtained at different mobile phase flow velocities at a constant gradient volume without optimi-

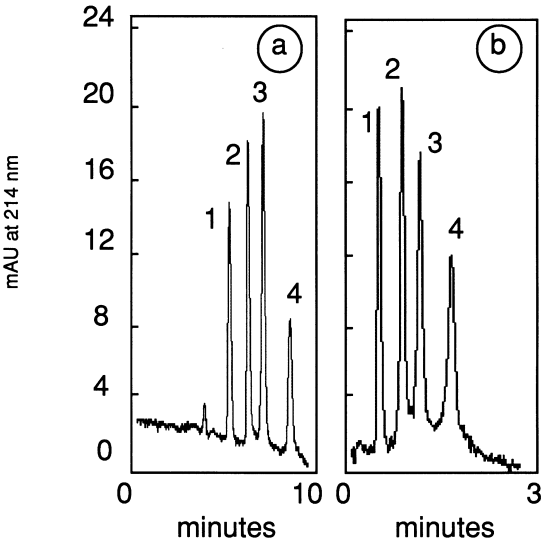

Fig. 9. Chromatogram of standard proteins obtained by μ-HPLC with a monolithic capillary column. Column I, 75 μm×27/38 cm, PS–DVB monolith; mobile phase, linear gradient from 20 to 75% acetonitrile in water containing 0.1% trifluoroacetic acid (TFA); sample: (1) ribonuclease A, (2) cytochrome *c*, (3) lysozyme, (4) β-lactoglobulin B (1 mg/ml of each in buffer). Flow-rate: (A) 0.34 μl/s, (B) 1.5 μl/s.

zation of the conditions. The results are promising because they indicate the potential of monolithic columns for fast separations at high flow velocities due to the relatively high porosity and the mechanical stability of the monolith.

5.2. Separation of peptides by CEC

In most applications to date, CEC has been used for the separation of small, neutral organic molecules under conditions of reversed-phase chromatography in high electric fields with EOF. When charged components are absent, electrophoretic migration of the sample components is not involved in the separation process. This is the reason why most of such CEC results can be treated within the hermeneutics of reversed-phase chromatography. On the other hand, a dramatically different picture may emerge when the sample contains both charged and neutral components because, in this case, the interplay of both chromatographic and electrophoretic forces gives form to the electrochromatogram. CEC can be considered either as an essentially chromatographic or an essentially electrophoretic process and the data can be processed according to the more appropriate framework. However, for the case when both mechanisms are important and act in concert, the theoretical treatment of the CEC process is yet to be established.

Insulin and three synthetic angiotensin-type peptides, whose amino acid sequences are given in Table 5, were separated isocratically on Column VI by counterdirectional CEC with reversed polarity. The styrenic surface of the stationary phase was functionalized with quaternary ammonium and *n*-octyl groups. The chromatograms in Fig. 10 show that both the acidic and basic sample components traverse the column in a single run at pH 3.0 in the order of increasing basicity. At first sight, this

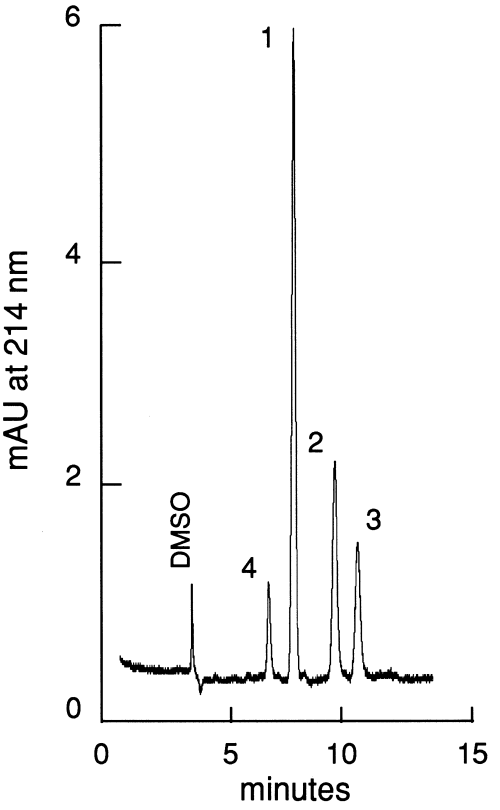

Fig. 10. Electrochromatogram of acidic and basic polypeptides. Conditions were the same as in Fig. 8. Applied voltage, −15 kV. Sample: (1) angiotensin II, (2) angiotensin I, (3) [Sar^1, Ala^8]-angiotensin II and (4) insulin; 4 mg/ml of each in buffer.

appears to be unexpected. On the other hand, the strong 'retention' of strongly basic peptides by the strongly basic stationary phase surface is due to an interplay of the EOF, hydrophobic retention, coulombic repulsion and the electrophoretic mobility of the sample components in the complex counterdirectional separation system.

The separation of peptides on a monolithic stationary phase containing alkyl-ammonium functions by

Table 5
Amino acid sequences of the angiotensins shown in the chromatogram in Fig. 10. The pK_a of peptides 1 and 2 is about 10.2. Values of pK_a and net charge were obtained from Hewlett-Packard, Technique, Publication No. 12-5968-1328E, 1999

Peak number	Angiotensin	Net charge
1	Asp–Arg–Val–Tyr–Ile–His–Pro–Phe	+2.65
2	Asp–Arg–Val–Tyr–Ile–His–Pro–Phe–His–Leu	+3.55
3	Sar–Arg–Val–Tyr–Ile–His–Pro–Ala	

counterdirectional CEC involves differential migration by both chromatographic and electrophoretic mechanisms. Consequently, the results are not expected to fit into the widely used schemes of reversed-phase chromatography and some of the chromatographic parameters have to be reevaluated. For instance, the dependence of the migration times of two angiotensins at three different acetonitrile concentrations is illustrated in Fig. 11. From the chromatograms, it can be inferred that the change in the migration rates with the ACN concentration is quite different from that typically found in conventional reversed-phase chromatography, as retention in this case increases with the organic strength of the mobile phase. For this reason, the linear relationships used traditionally to present retention data in reversed-phase chromatography, for instance, plots of log k' against the organic strength of the mobile phase, are not expected to hold when both chromatographic retention (thermodynamic process) and electrophoretic migration (kinetic process) together determine the overall migration velocities of the sample components. This is illustrated in Fig. 12 by plots of the migration times in Fig. 11 against the ACN concentration in the mobile phase. It is seen that the plots of both peptides go through first a maximum and then a minimum in the experimental concentration range of acetonitrile. As mentioned above, the migration times most remarkably increase with the organic modifier concentration in the acetonitrile concentration range from 25 to 40% (v/v). At 50% (v/v) ACN, the two peptides did not leave the column within 40 min. This cannot be explained by diminishing EOF velocity because it was found to change only slightly when the acetonitrile concentration was increased (not shown) to 75% (v/v).

Plots of the migration time of the two peptides against the salt concentration in the mobile phase containing 25% (v/v) acetonitrile are depicted in Fig. 13. It is seen that the migration times first go through

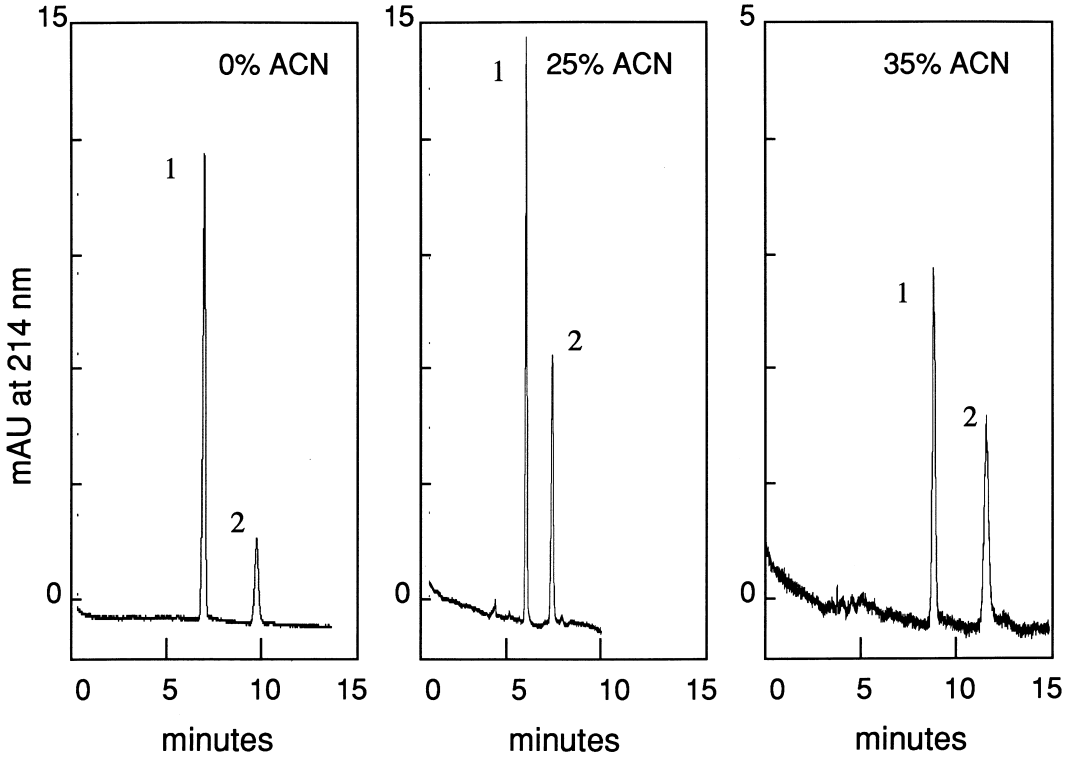

Fig. 11. Electrochromatograms of angiotensins obtained at different acetonitrile concentrations in the mobile phase. Conditions were the same as in Fig. 8. Applied voltage, −15 kV. Sample: (1) angiotensin II, (2) angiotensin I; 2 mg/ml of each in buffer.

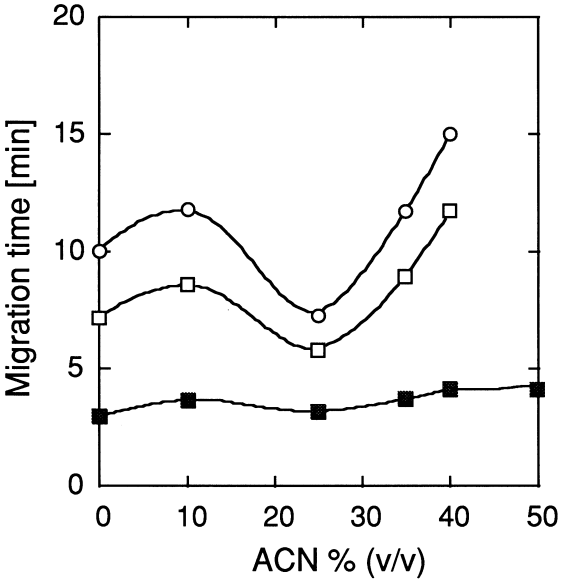

Fig. 12. Plots of the migration times of peptides and of the EOF marker DMSO (■) against acetonitrile concentration. Conditions were the same as in Fig. 8. Sample: DMSO (2 μl/ml dissolved in the mobile phase), angiotensin II (□) and angiotensin I (○); 2 mg/ml of each dissolved in mobile phase.

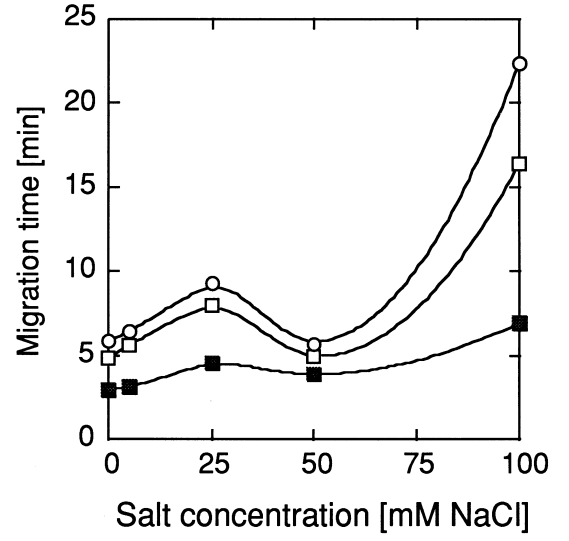

Fig. 13. Plots of the migration times of peptides and of DMSO (■) as the EOF marker against salt concentration. Conditions were the same as in Fig. 8. Sample: DMSO (2 μl/ml dissolved in the mobile phase), angiotensin II (□) and angiotensin I (○): 2 mg/ml of each dissolved in the mobile phase.

a maximum with increasing salt concentration then reach a minimum at 50 m*M* NaCl, after which, the migration times increase again with the salt concentration. The results in Fig. 13 show some vague similarity to the behavior described for retention in biopolymer chromatography with stationary phases having both fixed charges and hydrophobic binding sites [58]. The effect of salt concentration in the mobile phase on the migration time of the inert EOF tracer also presented in Fig. 13. As expected, the EOF velocity decreases with increasing salt concentrations.

We have also used monolithic capillary columns with unfunctionalized porous PS–DVB packing for the separation of two tripeptides, with neat phosphate buffer at neutral pH, and a typical chromatogram is depicted in Fig. 14. Upon addition of acetonitrile to the mobile phase, however, the EOF velocity, measured by electroosmotic mobility of the inert tracer, decreased significantly.

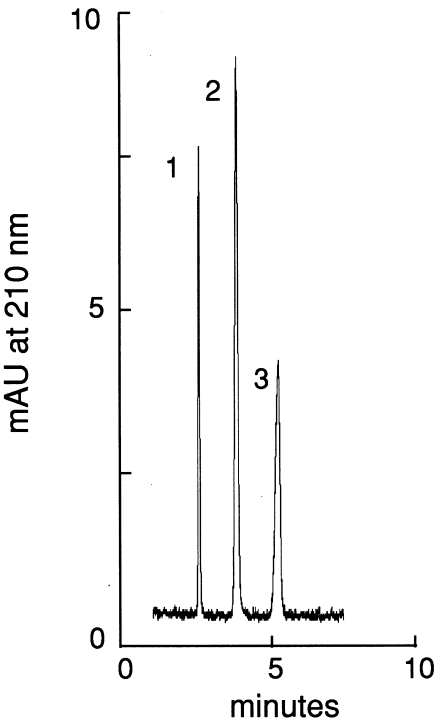

Fig. 14. Electrochromatogram of two tripeptides. Column I, 75 μm×27/38 cm unfunctionalized PS–DVB monolith. Sample: (1) thiourea (0.2 mg/ml), (2) Gly–Gly–Phe, (3) Phe–Gly–Gly; 2 mg/ml of each in water. Conditions were the same as in Fig. 7.

It is noted that the electrochromatographic separation process in the work presented here was not plagued by bubble formation, although both the inlet and outlet ends of the column were kept at atmospheric pressure. This observation confirms that siliceous retaining frits are at least in part responsible for bubble formation. Consequently, a significant advantage of monolithic column packings is that they do not require retaining frits.

6. Conclusion

The new platform, based on a porous monolithic packing, prepared from an in situ formed highly crosslinked poly(styrene–divinylbenzene) support, appears to be particularly well suited for engineering a new generation of capillary columns for use in CEC and μ-HPLC. The support is covalently attached to the presilanized capillary inner wall so that the conduit and the packing become an integral unit. The porous monolith provides a stable bed with good flow characteristics without the need for retaining frits, which are frequently blamed for bubble formation in CEC. The covalent anchoring of the monolith to the tube wall prevents the formation of a cleft, such as shown in Fig. 2A, between the tube wall and the polymeric packing. The outer part of the monoliths, which was prepared by our procedure, is a dense, fluid-impervious styrenic annulus that precludes contact between the silica surface and the aqueous buffer. The structure and other properties of the monolithic packing are readily controlled by the composition of the monomer mixture, the reaction time and the temperature. The porous structure of the packing is preferentially bimodal: larger channels for flow and smaller pores for adsorption. The pore structure and the permeability of the monolithic support, prepared with styrenic or acrylic monomers, can be easily controlled by selection of an appropriate porogen. In most cases, porous monolithic support is functionalized in situ in order to attach ionogenic functions and chromatographic binding sites to the surface. In principle, there is no restriction on further chemical modification of the stationary phase surface by well-established chemistries. The polymerization mixture is preferably of low viscosity in order to facilitate the filling of long capillaries, which, after polymerization and functionalization, can be cut to desired lengths. It is noted again that monolithic columns do not require retaining frits. The relatively high permeability of monolithic column packings can be of merit not only in CEC but also in high-speed μ-HPLC, as longer columns and mobile-phase velocities higher than those used conventionally can be employed. In CEC with particulate column packings, the integrity of the column is jeopardized in high electric fields by dislocation of the particles that have to be charged. In contrast, the monolithic nature of our column packings precludes such phenomena occurring so that they cannot engender untoward structural changes that drastically reduce the longevity of the column.

As mentioned before, CEC operation with monolithic columns does not suffer from bubble formation at moderately strong electric field strengths. Therefore, the system does not have to be pressurized in order to suppress the formation of bubbles. Consequently, not only porous-layer open-tubular columns, in which the porous monolith is simply an annulus at the inner wall of the capillary, but also fully packed monolithic columns, can be used in CEC when employed in equipment designed for CZE. Whereas the use of monolithic capillary columns is highly encouraging, much more research is still needed to establish optimal specifications and methods for reproducible preparation of columns that meet these specifications.

Acknowledgements

This work was supported by Grant No. 20933 from the National Institutes of Health, US Public Health Service. We are grateful to Dr. Ilya Tyomkin for help in liquid porosimetry measurements and to Dr. Reza Asiaie for his assistance with scanning electron microscopy.

References

[1] V. Pretorius, B.J. Hopkins, J.D. Schieke, J. Chromatogr. 99 (1974) 23.

[2] J.W. Jorgenson, K.D. Lukacs, J. Chromatogr. 218 (1981) 209.
[3] J.H. Knox, I.H. Grant, Chromatographia 32 (1991) 317.
[4] H. Yamamoto, J. Baumann, F. Erni, J. Chromatogr. 593 (1992) 313.
[5] H. Rebscher, U. Pyell, Chromatographia 38 (1994) 737.
[6] N.W. Smith, M.B. Evans, Chromatographia 38 (1994) 649.
[7] B. Behnke, E. Bayer, J. Chromatogr. A 680 (1994) 93.
[8] N.W. Smith, M.B. Evans, Chromatographia 41 (1995) 197.
[9] M.M. Dittmann, G.P. Rozing, J. Chromatogr. A 744 (1996) 63.
[10] G. Choudhary, Cs. Horváth, J. Chromatogr. A 781 (1997) 161.
[11] R.M. Seifar, W.Th. Kok, J.C. Kraak, H. Poppe, Chromatographia 46 (1997) 131.
[12] A.S. Lister, C.A. Rimmer, J.G. Dorsey, J. Chromatogr. A 828 (1998) 105.
[13] B. Xin, M.L. Lee, Electrophoresis 20 (1999) 67.
[14] A. Dermaux, P. Sandra, V. Ferraz, Electrophoresis 20 (1999) 74.
[15] Cs. Horváth, G. Choudhary, X. Huang, in: Proceedings of the 19th Int. Symp. on Capillary Chromatography and Electrophoresis, 1997, Wintergreen, VA, USA, 1997, p. 60.
[16] H. Watanabe, S. Kitagawa, M. Nakashima, T. Tsuda, Chromatography 15 (1994) 220.
[17] T. Tsuda, LC·GC Int. 5 (1992) 26.
[18] W.D. Pfeffer, E.S. Yeung, J. Chromatogr. 557 (1991) 125.
[19] Y. Guo, L.A. Colón, Anal. Chem. 67 (1995) 2511.
[20] J. Wu, P. Huang, M.X. Li, M.G. Qian, D.M. Lubman, Anal. Chem. 69 (1997) 320.
[21] H. Sawada, K. Jinno, Electrophoresis 20 (1999) 24.
[22] X. Huang, J. Zhang, Cs. Horváth, J. Chromatogr. A, in press.
[23] R. Asiaie, X. Huang, D. Farnan, Cs. Horváth, J. Chromatogr. A 806 (1998) 251.
[24] G. Chirica, V.T. Remcho, Electrophoresis 20 (1999) 50.
[25] A.I.M. Keulemans, in: A.B. Littlewood (Ed.), Gas Chromatography 1966, The Institute of Petroleum, London, 1967, p. 221.
[26] W.D. Ross, R.T. Jefferson, J. Chromatogr. Sci. 8 (1970) 386.
[27] F.D. Hileman, R.E. Sievers, G.G. Hess, W.D. Ross, Anal. Chem. 45 (1973) 1126.
[28] T.R. Lynn, D.R. Rushneck, A.R. Cooper, J. Chromatogr. Sci. 12 (1974) 76.
[29] S. Hjertén, J. Chromatogr. 473 (1989) 273.
[30] F. Švec, J.M.J. Fréchet, Anal. Chem. 64 (1992) 820.
[31] J. Matsui, T. Kato, T. Takeuchi, M. Suzuki, K. Yokoyama, E. Tamiya, I. Karube, Anal. Chem. 65 (1993) 2223.
[32] N. Minakuchi, K. Nakanishi, K.N. Soga, N. Ishizuka, N. Tanaka, Anal. Chem. 68 (1996) 3498.
[33] C. Fujimoto, Y. Fujise, Anal. Chem. 68 (1996) 2753.
[34] J.-L. Liao, C. Ericson, S. Hjertén, Anal. Chem. 68 (1996) 3468.
[35] C. Ericson, J.-L. Liao, K. Nakazato, S. Hjertén, J. Chromatogr. A 767 (1997) 33.
[36] E.C. Peters, M. Petro, F. Švec, J.M.J. Frèchet, Anal. Chem. 70 (1998) 2288.
[37] S.M. Fields, Anal. Chem. 68 (1996) 2709.
[38] M.T. Dulay, R.P. Kulkarni, R.N. Zare, Anal. Chem. 70 (1998) 5103.
[39] P.C. Carman, in: Flow of Gases Through Porous Media, Academic Press, New York, 1956, p. 42.
[40] B. Miller, I. Tyomkin, J. Coll. Interface Sci. 162 (1994) 163.
[41] K. Grob, in: Making and Manipulating Capillary Columns for Gas Chromatography, Hüthig, New York, 1986, p. 124.
[42] X. Huang, Cs. Horváth, J. Chromatogr. A 788 (1997) 155.
[43] L.L. Loyd, J. Chromatogr. 544 (1991) 201.
[44] M. von Smoluchowski, in: L. Graetz (Ed.), Handbuch der Elektrizität und des Magnetism, Verlag von Johann Ambrosius Barth, Leipzig, 1921, p. 366.
[45] Cs. Horváth, H.J. Lin, J. Chromatogr. 126 (1976) 401.
[46] J. Bear, in: Dynamics of Fluids in Porous Media, Dover Publications, New York, 1988, p. 113.
[47] R.E. de la Rue, C.W. Tobias, J. Eloctrochem. Soc. 106 (1959) 827.
[48] G.E. Archie, Trans. Am. Ind. Mining Met. Engrs. 146 (1942) 54.
[49] M.R.J. Wyllie, W.D. Rose, Nature 165 (1950) 972.
[50] W.O. Winsauer, H.M. Shearin, P.H. Masson, M. Willams, Bull. Am. Assoc. Petrol. Geologists 362 (1952) 253.
[51] A. Slawinski, J. Chim. Phys. 23 (1926) 710.
[52] J.W. Amyx, D.M. Bass, R.L. Whiting, in: Petroleum Reservoir Engineering, McGraw-Hill, New York, 1960, p. 68.
[53] P.C. Carman, Trans. Inst. Chem. Engrs., Lond. 15 (1937) 150.
[54] B.L. Karger, L.R. Snyder, Cs. Horváth, in: An Introduction to Separation Science, Wiley-Interscience, New York, 1973, p. 145.
[55] E. Wen, R. Asiaie, Cs. Horváth, J. Chromatogr. A, in press.
[56] P.A. Bristow, J.H. Knox, Chromatographia 10 (1977) 279.
[57] J.H. Knox, J. Cromatogr. Sci. 18 (1980) 453.
[58] W.R. Melander, Z. El Rassi, Cs. Horváth, J. Chromatogr. 469 (1989) 3.